Carbohydrate Polymers 86 (2011) 812–822

Contents lists available at ScienceDirect

Carbohydrate Polymers

journal homepage: www.elsevier.com/locate/carbpol

Films of arabinoxylans and β-glucans extracted from cereal grains: Molecular motions by TD-NMR

Ruifeng Ying, Luc Saulnier, Corinne Rondeau-Mouro*

UR1268 Biopolymères, Interactions, Assemblages, INRA, F-44316 Nantes, France

ARTICLE INFO

Article history:
Received 31 January 2011
Received in revised form 28 April 2011
Accepted 18 May 2011
Available online 26 May 2011

Keywords:
Arabinoxylans
β-Glucans
Cereal
Cell-walls
NMR
Polysaccharide
Water mobility

ABSTRACT

To mimic the lamellar organisation of polymers within cereal cell walls, films of arabinoxylan (AX) and β-glucan (BG) were prepared and characterized using Time-Domain (TD) ^{1}H NMR at different water contents and temperatures of measurement. The glass transition temperature (T_g) of the films was measured using differential scanning calorimetry (DSC). The investigation of M_2, i.e. the second moment of proton dipolar interactions, and T_2, i.e. the water spin–spin relaxation times, as a function of temperature and water content emphasized the complementary mechanisms involving the mobility of the polysaccharide chains both below and above the glass transition temperature, and the mobility of water molecules in interactions with the hydroxyl groups of the polysaccharides. In spite of the complexity of these mechanisms, we found that BG films featured higher M_2 values than AX films, which is consistent with higher proton intra- and inter-molecular dipolar interactions. These results, which are in agreement with the higher T_g obtained for BG films, were assigned to the smaller nanopores in the BG films which reduce the kinetics of the exchange between water molecules.

1. Introduction

The cell walls in wheat grain endosperm account only for 2–4% of the dry weight, but have a significant effect on wheat grain uses such as milling, baking, brewing and in animal feeding or human nutrition (Fincher & Stone, 1986). Arabinoxylans (AX) and mixed (1 → 3) (1 → 4)-β-D-glucans (BG) are the main components of the endosperm cell walls of cereal grains and represent around 70 and 30% of the walls, respectively (Fincher & Stone, 1986; Saulnier, Sado, Branlard, Charmet, & Guillon, 2007). The basic structure of AXs comprises a linear backbone of (1 → 4) linked β-D-xylopyranosyl (Xyl*p*) residues to which α-L-arabinofuranosyl (Ara*f*) substituents are attached through O-2 and/or O-3. AXs exhibit large natural variations in their structure mainly due to the degree of substitution of the xylose residues (i.e. either mono- or di-substituted) and the arabinose to xylose global ratio (A/X) with values ranging from 0.31 to 1.06 (Dervilly, Saulnier, Roger, & Thibault, 2000; Izydorczyk & Biliaderis, 1995; Saulnier et al., 2007). Some arabinose residues are esterified on the O-5 position mainly by ferulic acid (Izydorczyk & Biliaderis, 1995; Philippe, Tranquet, Utille, Saulnier, & Guillon, 2007). Mixed linkage (1 → 3, 1 → 4)-β-D-glucans, which are commonly known as β-glucans, are linear homopolymers of D-glucopyranosyl (Glc*p*) residues linked mostly via two or three consecutive β-(1 → 4) linkages that are separated by a single β-(1 → 3) linkage (MacGregor & Fincher, 1993). There is currently no evidence that two or more adjacent β-(1 → 3) linkages occur in β-glucan chains (Cui, Wood, Blackwell, & Nikiforuk, 2000; Dais & Perlin, 1982); the occurrence of large blocks of adjacent β-(1 → 4) linkages would most likely cause a tendency for inter-chain aggregation through strong hydrogen bonding along the cellulose-like regions. This property would potentially make the polymers less soluble in water (Izydorczyk, Macri, & MacGregor, 1998a, 1998b). Finally, BGs can be considered as a copolymers of 3-O-β-D-cellobiosyl-D-glucose and 3-O-β-D-cellotriosyl-D-glucose, which are tri- and tetra-saccharides, respectively, although longer blocks of consecutive β-(1 → 4) linkages are observed amongst the different sources of cereal BGs (Cui et al., 2000; Wood, Weisz, & Blackwell, 1991, 1994).

The local heterogeneity of the composition of endosperm cell walls has been investigated on samples recovered from fractionation processes (Ciacco & d'Appolonia, 1982) by the direct detection of fluorescence (Fulcher, Miller, & Ruan, 1997), coupling imaging and spectroscopic techniques (Barron, Parker, Mills, Rouau, & Wilson, 2005; Philippe, Barron, et al., 2006; Philippe, Robert, Barron, Saulnier, & Guillon, 2006), and immunolabelling techniques (Guillon et al., 2004; Philippe, Saulnier, & Guillon, 2006; Wood et al., 1994). It was concluded that BGs are present in a higher

Abbreviations: AX, Arabinoxylans; BG, β-glucans; DSC, differential scanning calorimetry; TD-NMR, Time-Domain nuclear magnetic resonance; T_g, glass transition temperature; RH, relative humidity.

* Corresponding author at: UR1268 Biopolymères, Interactions, Assemblages-INRA, Rue de la Géraudière, BP 71627, 44316 Nantes Cedex 3, France.
Tel.: +33 0 2 40 67 50 50; fax: +33 0 2 40 67 50 84.
E-mail addresses: corinne.rondeau@nantes.inra.fr, corinne.rondeau@cemagref.fr (C. Rondeau-Mouro).

0144-8617/$ – see front matter © 2011 Elsevier Ltd. All rights reserved.
doi:10.1016/j.carbpol.2011.05.033

proportion in the cell walls of the aleurone and subaleurone layers than in the starchy endosperm, which contains a higher content of AX in its central zone (Philippe, Saulnier, et al., 2006). Moreover, aleurone cell walls are characterized by a low A/X ratio in the range of 0.3–0.4 compared to 0.5–0.6 in the starchy endosperm cell walls. This chemical heterogeneity has been extensively described but little is known about the time-course and the pattern of AX and BG deposition in cell walls during endosperm development. Intermolecular interactions between the two polymers have also not been extensively explored although Izydorczyk and McGregor (2000) suggested that hydrogen bonding could occur between the two polymers if the lengths of uninterrupted β-(1 → 4)-glucan segments in BG and unsubstituted β-(1 → 4)-xylan in AX are sufficient.

Various observations using electron microscopy have shown a lamellar organisation in wheat endosperm cells walls that possibly reflects the assembly of the AX and BG polymers (Bacic & Stone, 1981; Guillon et al., 2004). In order to study the impact of their fine structures and interactions on primarily the hydration properties of cell walls, we prepared AX and BG films as models of the grain endosperm cell walls. We prepared a highly substituted AX with an A/X ratio of 0.73, which is consistent with the ratio determined for endosperm cell walls. Since BGs are present in wheat cell walls in a low amount and exhibit low water solubility possibly due to strong interchain interactions, we used commercial water-soluble BGs obtained from barley.

Herein, the Time-Domain (TD) ^{1}H NMR spectroscopy was chosen to investigate the mobility of the polymer chains and water in arabinoxylan and β-glucan films with different water contents as a function of temperature. In recent years, there has been an increasing interest in the use of Time-Domain ^{1}H NMR to study low-water-content food and biological materials (Cornillon & Salim, 2000; Rondeau-Mouro, Defer, Leboeuf, & Lahaye, 2008; Ruan & Chen, 1998). TD-NMR provides information not only about the molecular motion and state of water but also about the 'packing' of the protons in the solid phase via the second moment, M_2, of the dipolar interactions between protons (Aeberhardt, Bui, & Normand, 2007; Derbyshire et al., 2004; Kumagai, MacNaughtan, Farhat, & Mitchell, 2002; Partanen, Marie, MacNaughtan, Forssell, & Farhat, 2004; Van den Dries, Van Dusschoten, & Hemminga, 1998; Van den Dries, Van Dusschoten, Hemminga, & Van der Linden, 2000).

In the present study, the influence of both the water content and temperature on the mobility of water and the AX and BG chains within the films are discussed in relation to the structure of the molecules, their thermodynamic properties, and possible interactions through hydrogen bonding and the chemical exchange of protons with water molecules.

2. Materials and methods

2.1. Materials

Water-extractable arabinoxylans were prepared from wheat flours. The method of Dervilly-Pinel, Rimsten, Saulnier, Andersson, and Aman (2001) was used for the isolation of homogeneous AX fractions from wheat flour. The pure AXs (A/X = 0.73) were fractionated by graded ethanol precipitation, as was previously described (Dervilly et al., 2000). An ethanol concentration of 0.5% (v:v) was used in order to avoid the coprecipitation of AX chains due to their physical entanglement (Dervilly-Pinel et al., 2001). Barley water-soluble β-glucans (medium viscosity, purity >97%) were purchased from Megazyme.

2.2. Physicochemical analyses

The method of Englyst and Cummings (1988) was used to determine the composition of the monosaccharides. The polysaccharides were hydrolyzed with 2 N sulphuric acid at 100 °C for 2 h. Individual sugars were then converted to alditol acetates and analysed using gas-liquid chromatography (OV 225 column (30 m × 0.32 mm), 0.25 μm film thickness, FID detector at T = 230 °C). Analyses were made in duplicate (coefficients of variation <2%). The AX content was calculated from the sum the arabinose and xylose contents.

Protein contents were determined colorimetrically (Bradford, 1976) using BSA as the standard. The phenolic acid content in AX was determined by spectrophotometry as previously described by Saulnier, Vigouroux, and Thibault (1995).

Purified polysaccharides AX and BG were dissolved in deionised water (2 mg/mL) for 8 h at 60 °C with magnetic stirring and then filtered over a 0.45 μm membrane. The samples were injected at room temperature on a high-performance size-exclusion chromatography (HPSEC) system comprising two Shodex OH-pack SB HQ 804 and 805 columns eluted at 0.7 mL/min with 50 mM $NaNO_3$ containing 0.02% NaN_3. On-line molar mass and intrinsic viscosity determinations were performed at room temperature using a multi-angle laser-light scattering (MALLS) detector (mini-Dawn®, Wyatt, USA; operating at three angles: 41, 90 and 138°), a differential refractometer (ERC 7517 A) (dn/dc = 0.146 mL/g) and a differential viscometer (T-50A, Viscotek, USA). ASTRA 1.4 (Wyatt, USA) and TRISEC software were used to determine the weight average molar mass (M_w), the radius of gyration (R_G) and the intrinsic viscosity [η]. The polydispersity index, $I = M_w/M_n$, was calculated from the HPSEC-MALLS results.

2.3. Film preparation

The polysaccharides were dissolved in water (20 mg/mL) and 2.5 mL of each solution was cast into polystyrene Petri dishes (PS, Ø 5 cm, film thickness 10 μm). The films were dried in a climate room at 40 °C and 40% relative humidity (RH). Reflectance spectroscopy (SPECORD S 600) was used to determine the film thickness (Goodman, 1978).

The water sorption isotherms of the films were determined at 20 °C using the saturated salt method (Englyst & Cummings, 1988). The films were equilibrated at various water activities in desiccators containing saturated salt solutions with known RHs: LiCl (11%), NaBr (59%), NaCl (75%), and $BaCl_2$ (91%). The sorption of water was followed gravimetrically until equilibrium was achieved, which generally occurred within 15 days (Greenspan, 1977).

2.4. Differential scanning calorimetry (DSC)

The glass transition temperature, T_g, of the AX and BG films was measured using a DSC Q100 differential scanning calorimeter (TA Instrument) previously calibrated with indium. The films (20 mg) were equilibrated at the moisture contents considered in this work and then heated from −40 to 120 °C and from −40 to 150 °C at 3 °C/min. An empty pan was used as a reference and the glass transition temperature of the specimens was determined from the midpoint of the heat capacity change observed during the second scan.

2.5. NMR measurements

^{1}H NMR measurements were performed using a Time-Domain spectrometer (Minispec BRUKER, GERMANY) operating at a resonance frequency of 20 MHz. The NMR system was equipped with a temperature control device connected to a calibrated optic fibre (Neoptix Inc., Canada) allowing for ±0.1 °C temperature regulation. The AX and BG films (film thickness 10 μm, Ø 8 mm) were inserted into a 10 mm diameter glass tube. The tubes were filled to about 10 mm in height in order to place the samples within the homogeneous region of the NMR magnet then weighed and hermetically

closed. A Teflon rod was used to fill the dead volume of each tube to avoid water loss. Thermal equilibration was ensured by allowing a 7 min waiting time after each temperature step before the experiment was started. The samples at various water contents were analysed at temperatures ranging from −40 to 80 °C at increment of 5 °C. The regulation of temperature was carried out using liquid nitrogen; higher temperatures would have required another regulation system, which was unavailable during testing. Two types of pulse sequences were used. Proton free induction decays (FID) were acquired using the following parameters: a 90° pulse of 3.2 μs, a dwell time of 0.5 μs between two successive data points, 160 scans of 19,900 data points, and a recycle delay of 2 s between each scan. The Carr–Purcell–Meiboom–Gill (CPMG) pulse sequence was used with a delay between the 90° and 180° pulses of 40 μs. 160 scans were acquired with 800 data points (Meiboom & Gill, 1958).

The second moment, M_2, values were calculated from the broad part of the FID curve that arose due to the protons of the solid fraction. As pointed out by Abragam (1961), the NMR spectrum of these protons is well represented by a combination of a sinus function and a Gaussian broadening following Eq. (1):

$$I_{FID}(t) = A \exp\left(-\frac{a^2t^2}{2}\right)\frac{\sin bt}{bt} + B \exp\left(-\frac{t}{T_2^*}\right) \quad (1)$$

In this equation, parameters A and B represent the contributions of the immobile and mobile protons in the sample, respectively. The NMR spectrum of the immobile proton fraction is assumed to have a rectangular line shape with a total width of 2*b*, which is convoluted with a Gaussian line shape with a standard deviation given by parameter *a*. The second moment, which is a measure of the strength of the dipolar interaction of the hydrogen atoms (for details, see Section 3), is calculated from the fit parameters *a* and *b* using Eq. (2).

$$M_2 = a^2 + \frac{1}{3}b^2 \quad (2)$$

The mobile fraction (B) should display a lower limiting value of T_2^* around 1.3×10^{-6} s, which is approximately 2*b* and corresponds to an upper limit of the rotation correlation time, τ_c, of 5×10^{-5} s, as calculated using the Bloembergen–Purcell–Pound theory (Bloembergen, Purcell, & Pound, 1948). Protons with τ_c values higher than 5×10^{-5} s are deemed immobile and belong in the A fraction.

Transverse relaxation data were analysed with the following model:

$$I_{CPMG}(t) = \sum_{i=i}^{i} A_i \times \exp\left(-\frac{t}{T_{2i}}\right) \quad (3)$$

where T_{2i} are the relaxation times of the mobile populations and A_i is the intensity of the mobile populations (Meiboom & Gill, 1958). To ensure the accuracy of the data treatment, spin–spin relaxation decay curves were fitted using CONTIN (Provencher, 1982) and a discrete method (Marquardt, 1963).

For the sake of clarity, three NMR parameters must be defined: (i) T_{2TP} is the maximum value of T_2 when varying the temperature of the measurement (T_2 on top of the peak), (ii) T_{T_2} is the transition temperature for T_2, and (iii) T_{M_2} is the transition temperature for M_2 when is measured as a function of temperature.

Table 1
Molecular characteristics of AX and BG. Weight average molar mass (M_W), radius of gyration (R_G), polydispersity index (I), intrinsic viscosity ([η]) and arabinose to xylose ratio (Ara/Xyl).

Samples	$M_w \times 10$ (g mol^{-1})	R_G (nm)	I	[η] (mL/g)	Ara/Xyl
AX	233.2	34	2.4	259.64	0.73
BG	283.5	31	1.5	331.2	

3. Results and discussion

3.1. Structural and physicochemical characterizations

Table 1 shows the molar mass, the radius of gyration and the intrinsic viscosity of AX and BG. While the average molecular weights and intrinsic viscosities were similar, the polydispersity index of AX was higher than that of BG. The protein contents of AX and BG were 3.0% and 0.1%, respectively. In addition, AX contained 0.16% ferulic acid esterified to the arabinose side chains. The degree of substitution of the xylan backbone by arabinose residues (A/X ratio: 0.73) was in the upper range of that observed for wheat endosperm AX (Dervilly et al., 2000; Hoffmann, Roza, Maat, Kamerling, & Vliegenthart, 1991; Izydorczyk & Biliaderis, 1995; Rattan, Izydorczyk, & Biliaderis, 1994).

The majority of Ara*f* residues were disubstituted xylose residues (29.3% of the xylan backbone as estimated by liquid ^{1}H NMR, not shown), while monosubstituted and unsubstituted xyloses represented 14.4% and 56.3%, respectively, of the xylan backbone. The relative proportion of disubstitution and monosubstitution of the xylose residues in the xylan backbone reflect a non-random process of the biosynthetic mechanisms favouring disubstitution (Dervilly-Pinel, Tran, & Saulnier, 2004). However, the random or non-random arrangement of substitution along the xylan chains is not clearly established. Tentative structural models support an irregular distribution of the arabinose substituents with possible blocks of contiguously unsubstituted Xyl*p* (Fig. 1), and their proportions and lengths vary according to the A/X ratio (Dervilly et al., 2000; Izydorczyk & Biliaderis, 1994, 1995; Saulnier et al., 2007). It has been shown that for low-substituted AX (A/X ≤ 0.3), the regions of contiguous unsubstituted xylan chains potentially interact together through hydrogen bonding and contribute to crystallization between the xylan chains (Hoije, Sternemalm, Heikkinen, Tenkanen, & Gatenholm, 2008). For highly substituted AX, the arabinose side-chains prevent molecular interactions and crystallization between the xylan chains (Hoije et al., 2008). In our AX sample (A/X = 0.73), regions of contiguous unsubstituted xylose residues are not abundant which limits the hydrogen bonding between β-(1 → 4)-xylans in agreement with the amorphous state of the films that was revealed by X-ray diffraction (results not shown).

The β-glucan chains comprised 3-O-β-D-cellobiosyl-D-glucose (trisaccharide unit, DP 3) and 3-O-β-D-cellotriosyl-D-glucose (tetrasaccharide unit, DP 4) which accounted for 90–95% of the total oligosaccharides, and longer oligosaccharides (DP5-6) which accounted for 5–10% of the total (Fig. 2) (Wood et al., 1991, 1994). Despite the non-random arrangement of the individual (1 → 3) and (1 → 4)-β-linkages, the cellotriosyl (G3), cellotetraosyl (G4), and longer cello-oligomers were arranged in an essentially independent

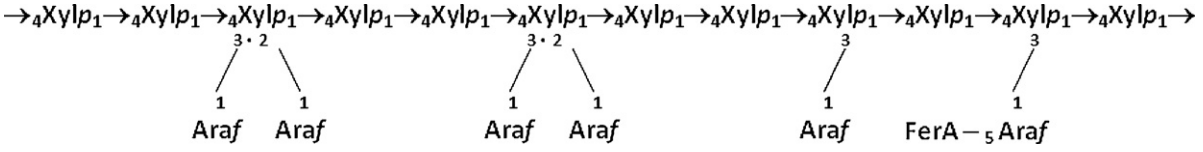

Fig. 1. Structure of arabinoxylans (Ara*f*: arabinofuranose, Xyl*p*: xylopyranose, FerA: ferulic acid).

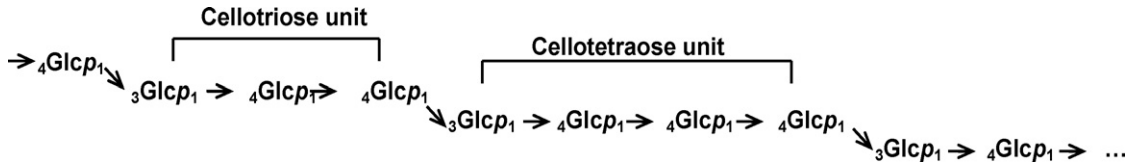

Fig. 2. General molecular structure of β-glucans (Glc*p*: glucose).

and random fashion in the β-glucan chains (Buliga, Brant, & Fincher, 1986; Staudte, Woodward, Fincher, & Stone, 1983). The G3/G4 molar ratio is a characteristic that distinguishes β-glucans from various sources (Cui et al., 2000; Izydorczyk et al., 1998a, 1998b; Wood et al., 1991, 1994); the molar ratio of barley BG is usually between 2.8 and 3.3 (Izydorczyk et al., 1998a, 1998b; Wood et al., 1991, 1994). The X-ray diffractograms acquired for the BG films were consistent with an amorphous state (results not shown), but the G3/G4 molar ratio of around 3 suggests possible conformational regularity in BG through hydrogen bonding between long blocks of contiguous cellotriosyl fragments (Izawa, Kano, & Koshino, 1993). This inter-chain interaction could affect the solubility of BG, but did not give rise to stable crystalline structures as was supposed by Tvaroska, Ogawa, Deslandes, and Marchessault (1983).

In addition to their different molecular structures, AX and BG exhibit different physicochemical characteristics. The two first columns of Table 2 indicate the water content and the glass transition temperature of AX and BG films prepared at different relative humidities. The water content increased with increasing RH within the AX and BG films. For RHs between 11 and 75%, the BG films contained more water than the AX films; however, at an RH of 91%, the tendency was inversed. The T_g of the AX and BG films decreased as the water content increased due to the plasticising effect of water (Roos & Karel, 1990; Van den Dries et al., 1998). The T_g values of the AX and BG films were much higher than those of monosaccharides such as glucose (Van den Dries, Besseling, Van Dusschoten, Hemminga, & Van der Linden, 2000), disaccharides such as maltose (Van den Dries et al., 1998), and oligosaccharides such as maltodextrin (Kilburn, Claude, Schweizer, Alam, & Ubbink, 2005) for the same water content. However, they were similar to the value observed for polysaccharides such as starch (Roudaut, Farhat, Poirier-Brulez, & Champion, 2009). The T_g values were higher for the BG films than for the AX films when the water content was between 3 and 35%.

The molecular processes that contribute to the glass transition temperature are currently the subject of intensive research and debate. Whether the changes in thermodynamic properties (e.g. specific heat and volume) that are seen during cooling (or reheating) are due to a real thermodynamic phase transition or are of purely kinetic origin is a controversial issue, and no theory has yet been proposed which accounts for all of the observed experimental features. Several excellent reviews that describe the current thinking in this field have been published (Ediger, Angell, & Nagel, 1996; Mansfield, 1993). Models based on statistical mechanical or free-volume theories are the simplest and most widely invoked and depend on molecular motion in relation to the medium viscosity. Therefore, the difference of the glass transition temperature between the BG and AX films could be linked to the different motions of the polymer chains. We studied the molecular mobility of water and polysaccharide protons in AX and BG films as a function of water content and temperature using ^{1}H NMR.

3.2. NMR analyses

The study of the free-induction decay (FID) observed for these films indicated an oscillation (or a beat) of the NMR signal arising from residual local orders within the films. This short-range organisation induces strong dipolar interactions between protons which are characterized by the second moment, M_2 (Aeberhardt et al., 2007; Derbyshire et al., 2004; Kumagai et al., 2002; Partanen et al., 2004; Van den Dries et al., 1998; Van den Dries, Van Dusschoten, et al., 2000). This informs about the polysaccharide motions in relation to the dipolar interactions between chains and the nanostructure of the films.

M_2 values should originate from two contributions: one corresponds to the intramolecular dipolar interactions which are modulated by local proton mobility and their inter-distances within molecules (within polysaccharide chains), and the other is due to intermolecular dipolar interactions that are dependent on the motion of the chains and the average distance between the polysaccharide chains. These contributions were easily observed in the FID signals recorded at 20 °C for the AX and BG films (Fig. 3a and b). The oscillations were observed at short times for the dried samples (0% water). The sinusoidal pattern observed in the FIDs has already been depicted in glassy oligosaccharides such as maltose (Aeberhardt et al., 2007; Derbyshire et al., 2004; Van den Dries et al., 1998; Van den Dries, Van Dusschoten, et al., 2000) or starch (Kumagai et al., 2002; Partanen et al., 2004; Roudaut et al., 2009). The fast decay of the signal was caused by the protons of the rigid phase (polysaccharides), whereas the slow decay is related to the mobile protons of the liquid water phase (Abragam, 1961). As the water content of samples increased, the FID beat pattern was less pronounced as a consequence of a decrease in the number and/or strength of the dipolar interactions within the AX and BG films (Fig. 3). At a higher water content, the small beat of the FID signal for AX films disappeared while it remained for the highly hydrated BG films. This observation emphasizes the different hydration behaviour of AX as compared to BG films. This phenomenon could result from: (i) a reduction of the proton density, (ii) an increase of the proton distances, and/or (iii) an improvement of the anisotropic mobility of the polysaccharide chains which in

Table 2
Values of water content (%), glass transition temperature (T_g), transition temperatures from M_2 (T_{M_2}), transition temperatures from T_2 (T_{T_2}) and corresponding T_2 values (T_{2TP}) for AX and BG films prepared at different RH.

RH (%)	AX films					BG films				
	Water content (%)	T_g[a] (°C)	T_{M_2} (°C)	T_{T_2} (°C)	T_{2TP} (ms)	Water content (%)	T_g[a] (°C)	T_{M_2} (°C)	T_{T_2} (°C)	T_{2TP} (ms)
11%	3.50%	>80	0	>80	nd	4.71%	nd	0	>80	nd
59%	15.24%	82	nd	60	7.8	16.43%	101	nd	65	3.62
75%	17.82%	56	60	50	8.98	19.40%	71	nd	55	3.65
91%	34.17%	−6	−5; 60	20	12.05	28.86%	29	50	35	4.47

[a] T_g (onset) determined from the 2nd heating run (at 3 °C/min).

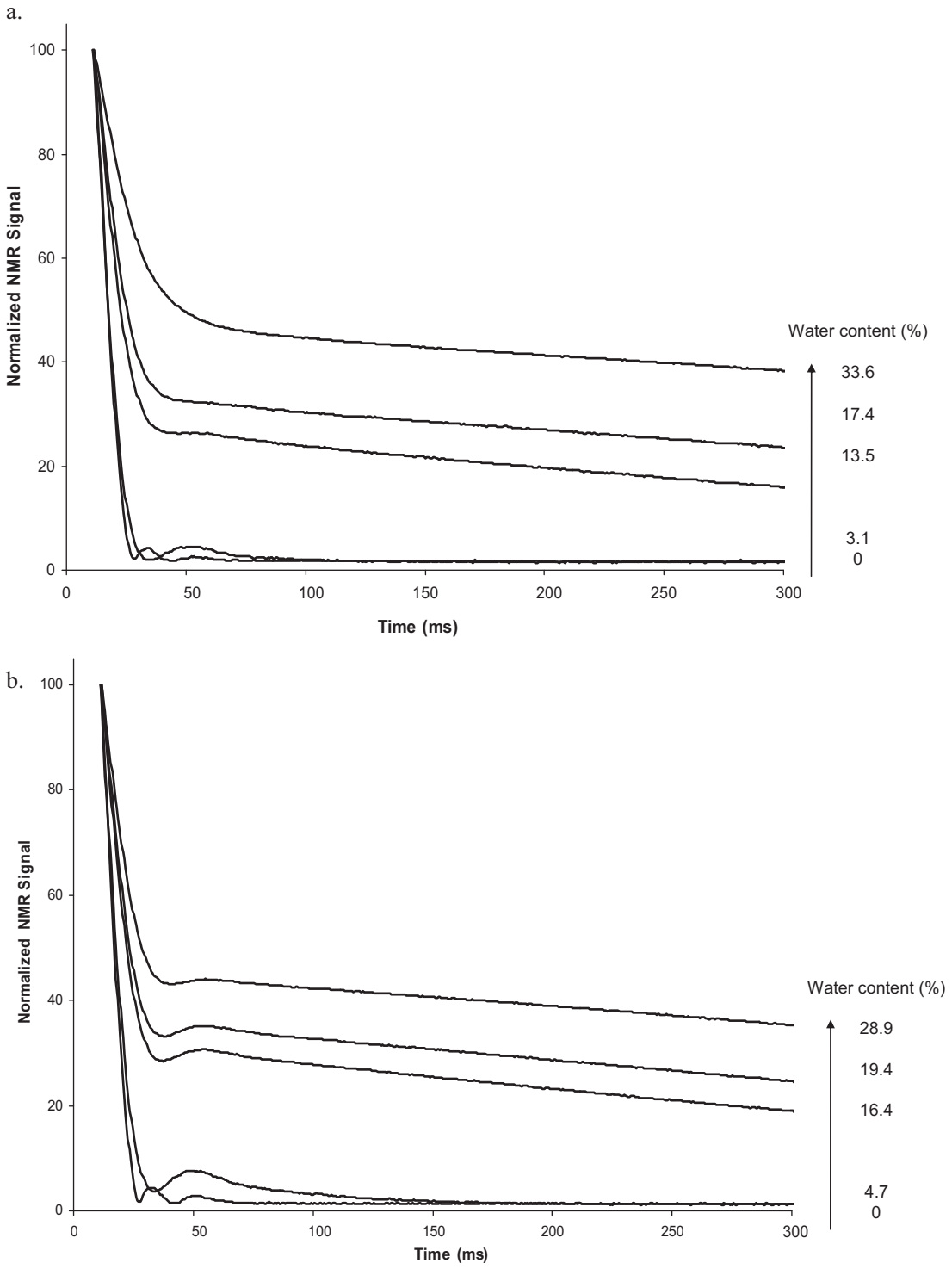

Fig. 3. FID signal of AX (a) and BG (b) films with different water contents at 20 °C.

the same time diffuse more rapidly. The source of this phenomenon, which seems to vary from one polysaccharide type to another, can be investigated by calculating the second moment values, M_2, and measuring the water spin–spin relaxation times, T_2, as a function of the water content and temperature variations.

3.3. Second moment M_2 of dipolar interactions

The fitting of Eq. (1) permitted the calculation of the second moment, M_2, values as a function of parameters a and b following Eq. (2) (see Section 2). The results are compiled in Fig. 4 showing the effects of both water content and temperature on M_2 within the AX and BG films. M_2 evolved linearly with temperature as already shown for the various carbohydrate materials and mixtures in their glassy state (Derbyshire et al., 2004; Kumagai et al., 2002; Van den Dries et al., 2000). At certain temperatures (referred to as T_{M_2}), breaks in M_2 were observed with a consequent change in the linear slope of M_2 versus temperature. A comparison of the slopes of the linear variation of M_2 versus temperature indicated changes which depend on the structure of the polysaccharide as well as their

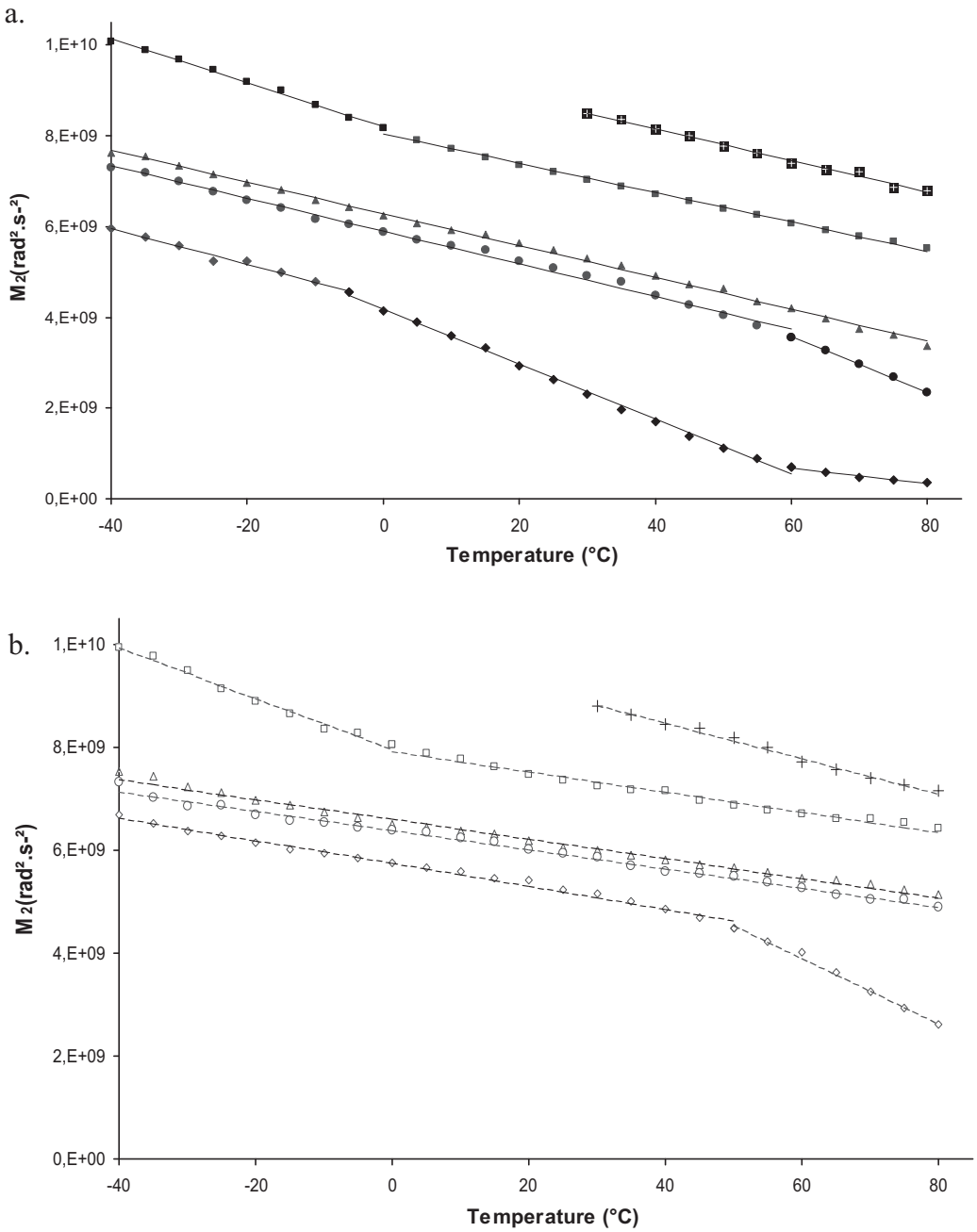

Fig. 4. Effect of temperature and water content on the second moment (M_2) for AX films (a) white cross = 0% (P_2O_5); filled cubes RH = 11%; filled triangles RH = 59%; filled circles RH = 75%; filled diamonds RH = 91%; and for BG films (b) black cross = 0% (P_2O_5); open cubes RH = 11%; open triangles RH = 59%; open circles RH = 75%; open diamonds RH = 91%.

glassy–rubbery transition. This observation is consistent with published results which showed that the slope of M_2 as a function of (T–T_g) evolves with the type of oligosaccharide (Aeberhardt et al., 2007). Dried films of AX and BG (0% water content) were characterized by similarly high M_2 values ($>8 \times 10^{+9}$ rad^2 s^{-2}) and slopes consistent with strong dipolar interactions between polysaccharide protons potentially through hydrogen bonding without bridging water molecules. Fig. 4 indicates that lower measured M_2 values correlated with higher water content. The decrease of M_2 with an increase in water content indicated a lower proton dipolar strength or a lower proton density due to an increase in the mobility and/or average distances of the polysaccharide protons (Van den Dries, Van Dusschoten, et al., 2000). However, as the water content of the samples increased, the intensity of the FID signal (A + B from Eq. (1)) improved which is in support of the fact that proton density was higher for water than for polysaccharides (namely 2/18 for water, compared to 8/132 and 10/162 for AX and BG respectively). Therefore, the impact of water on M_2 could not be linked to lower proton density. Moreover, at −40 °C below the T_g values of the polysaccharide films, the intra-molecular contributions in samples should remain constant regardless of the water content. Therefore, the changes in the M_2 values are related to variations of the intermolecular interactions that are modulated only by the average distances between the protons of the polysaccharides since their proton mobility was extremely reduced. Thus, at −40 °C, the decrease of M_2 as a function of water content indicated higher average distances between the polysaccharide chains (Van den Dries, Besseling, et al., 2000).

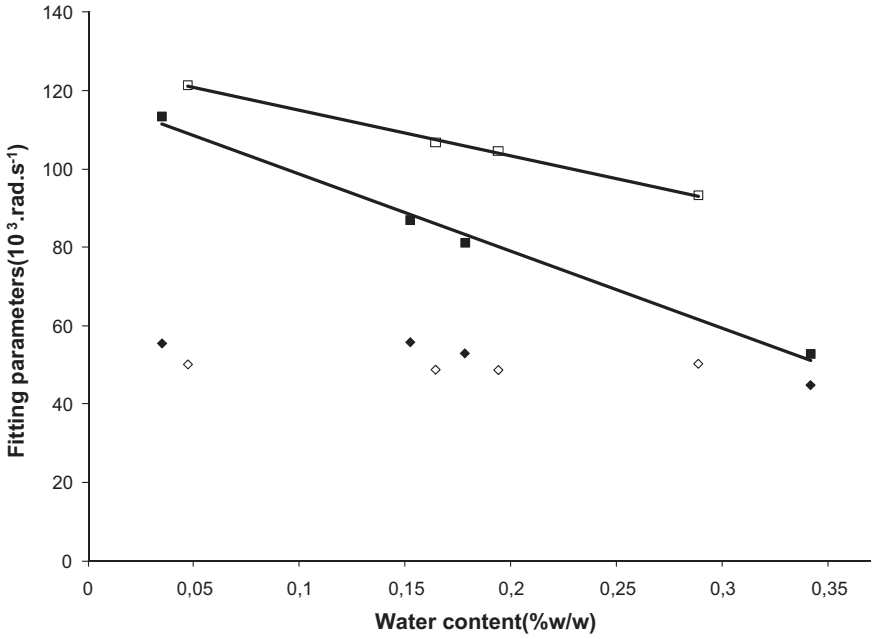

Fig. 5. Linear variation against water content of the parameters *a* (diamonds) and *b* (cubes) from Eq. (2), calculated for AX films (filled symbols) and BG films (open symbols) at 20 °C.

After increasing the water content within films to between 3 and 20%, few breaks of slope were observed below 0 °C. A comparison of the slopes of M_2 versus temperature for the AX and BG films also indicated few variations within the nature of the polysaccharides. This observation indicates that below 0 °C the protons of the arabinose residues were as immobile as the xylose and glucose protons. The dipolar interactions were modulated only by the water content which affected the average proton distances.

In order to more precisely investigate the variation of M_2 relative to the water content, it was possible to analyze the changes of parameters *a* and *b*, which were estimated from Eq. (2). Fig. 5 shows the changes in parameters *a* and *b* with the water content of the films at 20 °C. Parameters *a* and *b* depend on the strength of the dipolar interactions (Abragam, 1961) in solid samples and are related to one another through molecular structures and molecular assemblies (non-random molecular motions) (Derbyshire et al., 2004). The spin–spin relaxation, T_{21}, of the low-mobility phase is proportional to *a* following the relation $T_{21} = \sqrt{2/a}$ in which *a* is characteristic of the energy involved in the average interaction between protons (i.e. the protons of the OH and CH moieties of the polysaccharide molecules), whereas *b* depends on both the number of interactions and the distance between these dipoles (Abragam, 1961).

The calculation of T_{21} at 20 °C gave values varying from 25.3 to 31.6 μs, which are close to the values obtained for different oligosaccharides at various hydration levels (Aeberhardt et al., 2007). This result suggests that, under certain thermal conditions, T_{21} can be considered to be independent of the nature of the oligosaccharides. Indeed, as shown in Fig. 5, *b* decreased linearly as the water content increased, whereas *a* remained relatively constant except for AX films with a water content >35% for which *a* began to decrease, which was confirmed at higher temperatures (not shown). Therefore, as long as the temperature was lower than the T_g of the polysaccharide films, the motion of the polysaccharide protons was reduced and *a* remained constant regardless of the hydration level assuming no effect of water on this parameter (i.e. no 'solid water'). However, given that the addition of water increased the mobility of the solid phase protons (i.e. the protons of the CH and OH moieties of the polysaccharides) above the T_g presumably by increasing the proton exchange frequency, a higher relaxation time of these protons, i.e. a decrease in *a*, should have been observed as the water content was increased. The decay time, *b*, decreased with increasing water content and, at a very high hydration level, the damped oscillations characteristic of the solid phase disappeared, as seen in Fig. 3a and b. At a high water content, the molecular motions became so important that the intermolecular interactions average giving rise to the loss of 'non random' structures (Abragam, 1961). A comparison between the two kinds of films indicated that the values of *b* were higher for BG films with a less pronounced decrease when water content increased. These results were confirmed by the variations of M_2 at temperature below 50 °C, as seen in Fig. 4. For water contents between 3 and 20% (RH = 11–75) and temperatures varying from 0 to 50 °C (therefore, below T_g) few changes in the slopes were noted for films made using the same polysaccharide. Nevertheless, the M_2 values of the BG films were higher and the slopes weaker as compared to those of the AX films. These results are consistent with the measured T_g values which were higher for the BG films and must be connected with stronger dipolar interactions between protons due to the shorter average distances between the protons of the polysaccharide chains within the BG films. Therefore, for samples below 50 °C with low water content, changes in M_2 can be related to the differences in the motion of the polysaccharide protons and/or their average distances in relation with: (i) the chemical structure of the polysaccharides, and (ii) the assemblies of the polysaccharides within films.

In AX and BG, the xylose and glucose residues are attached through two glycosidic bonds per residue (except for the reducing ends) while the arabinose residues are attached to the linear backbone by a single linkage per residue. Therefore, the xylose and glucose residues should be less mobile than the arabinose residues, thereby inducing a larger average mobility of the ring protons of arabinose in AX films. Moreover, the interproton distance gap can be explained by the polysaccharide structure (Figs. 1 and 2). Compared to the smooth chains of BG, AX features branched polymers of xylose that contain 73% arabinose substituents of which 14.6% of them are bound to xylose residues in position O-3 and 29.3% in position O-3 and O-2 (as determined by high-field ^{1}H NMR). The

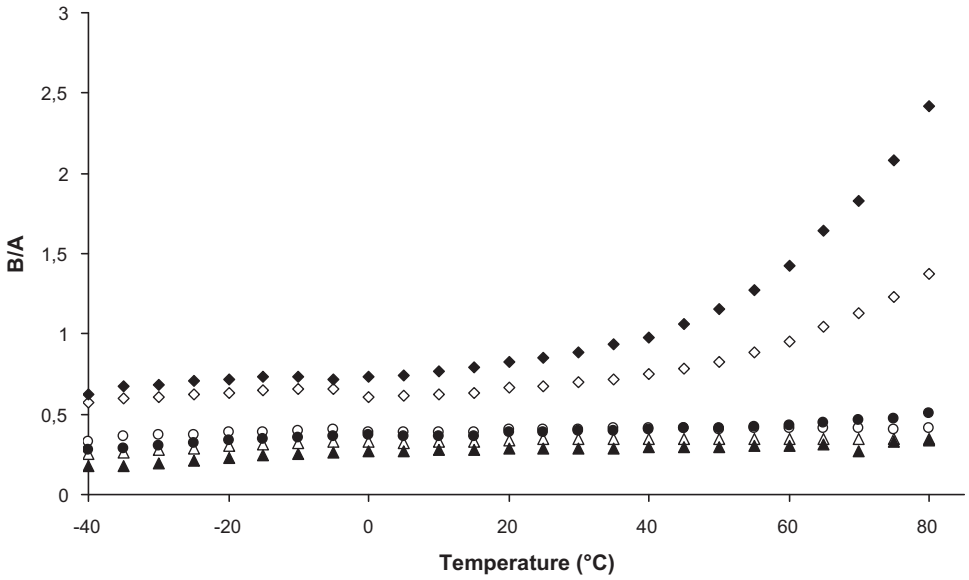

Fig. 6. Ratio of the mobile (B) and immobile (A) proton fractions as function of temperature for AX films (filled triangles RH = 59%; filled circles RH = 75%; filled diamonds RH = 91%) and BG films (open triangles RH = 59%; open circles RH = 75%; open diamonds RH = 91%).

steric hindrance of the arabinose branch points explains the larger interproton distances, which could enlarge as the temperature is increased.

Comparison of the breaks in M_2 (T_{M_2} in Table 2) indicated that, in the rubbery state, the protons of the polysaccharides (exchangeable and non-exchangeable) as well as the polysaccharide chains become very mobile which induces the melting of the hydrogen-bond network and then a significant decrease in M_2. However, in the glass state, some differences in the T_{M_2} values and the transition temperatures determined by DSC were observed. A transition temperature of around 0 °C was measured for the samples with low hydration (RH = 11%) while the T_g could not be determined for this hydration state and was assumed to be higher than 100 °C. This transition could originate from the ice melting which would contribute to the intermolecular dipolar interactions. This hypothesis is surprising considering that the hydration level of these films is <5%. Moreover, Fig. 6 shows the ratios of the mobile (B) and immobile (A) proton fractions, which were determined using Eq. (1), as a function of temperature within the films for water contents between 3 and 35%. There was no evidence of an increase in B/A between −40 °C and 0 °C regardless of the water content of the films. The transition temperature at 0 °C may be due to a loosening of the intra-molecular dipolar interactions between the protons of the polysaccharides above 0 °C. The measurement of this transition using low-field NMR when no such transition was detectable by DSC can be explained by the different time scale of the measurements: the rate of temperature change in DSC corresponds with a glass-transition time scale of seconds while NMR measures the motion of polysaccharides with correlation times on the microsecond scale. Other breaks in the slope of M_2 versus temperature were observed for higher water contents. A transition was estimated at around 60 °C for AX films prepared at RH = 75%, which is close to the T_g value of 56 °C determined by DSC. This transition was also present for AX films prepared at RH = 91% in addition to a transition at around −5 °C, which is also close to the T_g value of −6 °C determined for this film. The presence of the second transition around 60 °C, which is close to the T_g for AX films prepared at RH = 75%, may originate from a hydration heterogeneity or a dehydration of the AX films prepared at RH = 91%. The T_{M_2} of BG films with a water content of 28.9% (RH = 91%) was estimated to be 50 °C, which is 21 °C higher than the T_g value. As for the AX films, either the hydration of the films was not homogeneous or another phenomenon resulted in the transition at a higher temperature. Van den Dries, Besseling, et al. (2000) have explained that this additional transition is caused by an abrupt decrease in viscosity above the T_g due to collapse phenomenon. This phenomenon has been observed by DSC, light scattering, and viscosity measurements for very high molecular weight polymers at very low concentrations (Roos & Karel, 1990; Roos, 2002; Sato, Sakurai, Norisuye, & Fujita, 1983). The collapse transition is generally considered to be a rearrangement through the intramolecular hydrogen bonds of the polymer chains from an open coil to a compact ball either due to lower temperatures or deterioration in the solvent quality.

3.4. Water relaxation time T_2

Measurements of spin–spin relaxation times, T_2, of the water protons within films were carried out as a function of temperature. As shown in Fig. 7, the T_2 values increased from −40 °C to a maximum value (on top of the peak noted T_{2TP}) at a temperature of T_{T_2} which varies depending on the composition and hydration state of the films (Table 2). For temperatures above T_{T_2}, a decrease in T_2 was observed. This decrease could be explained by Gottwald, Creamer, Hubbard, and Callaghan (2005); (i) additional molecular diffusion processes of water, (ii) averaging due to additional rapid motions of the polysaccharide protons, or (iii) averaging due to rapid chemical exchanges of water molecules between a free state and being bound to the hydroxyl groups of the polysaccharides (the so-called fluctuations of the Larmor frequencies).

The T_2 values for the AX and BG films (see Table 2) were similar at a low water content (<5%) while the AX films displayed higher T_2 values than the BG films at water contents between 15 and 35%, which suggests that the rotational mobility and exchange of water were slower in the BG films. In the present work, the systems have to be considered relative to the glassy and rubbery states of the polysaccharide-constituting films (determined by the transition temperature T_g) as well as to the frequency of the water exchanges which depend not only on the temperature but also on the microporosity of the films.

Considering the results gathered in Fig. 7 and Table 2, the first observation is that the T_2 values increased as the temperature rose up to T_{T_2}. This phenomenon is easily explained by the decrease of τc

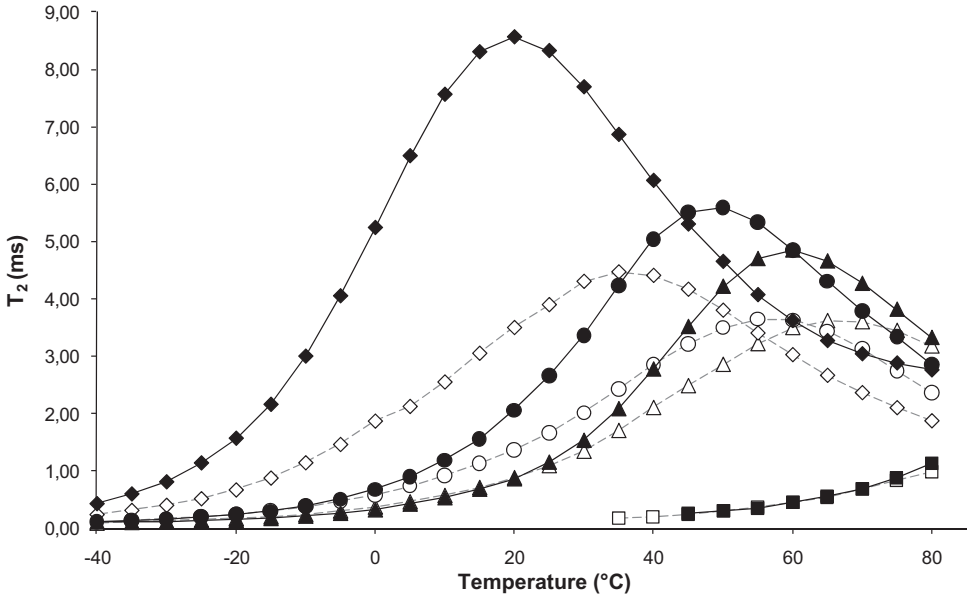

Fig. 7. Effect of temperature on T_2 (relaxation time) for AX films (filled cubes RH = 11%; filled triangles RH = 59%; filled circles RH = 75%; filled diamonds RH = 91%) and BG films (open cubes RH = 11%; open triangles RH = 59%; open circles RH = 75%; open diamonds RH = 91%).

when the temperature increases, which occurs concomitantly with a decrease in the proton dipolar interactions since the frequency of proton exchange rises. The second result is that the T_2 values increased with the water content in the AX films (see values of T_{2TP} in Table 2); however, this is dependent on the nature of the polysaccharide since few variations of T_2 were observed within the BG films. The BG films had lower T_2 values than those of the AX films, which is consistent with faster proton exchange between the bulky and solid phases of the BG films in relation to the smaller global nanoporosity within the BG films.

For water contents between 15 and 35%, the T_{T_2} values were greater for BG than for AX which is in agreement with the differences observed for T_g and T_{M_2} (Table 2). The higher temperatures of transition and lower T_2 values are consistent with the stronger dipolar interactions of the protons in the polymers of the BG films due to the smaller chain inter-distance in the BG films as opposed to the AX films which is related to the respectively linear and branched structures of the two polymers, as was previously explained (see M_2 variations).

However, for both polymers the T_{T_2} values were lower than the T_g and T_{M_2} values for water contents between 15 and 20%, while above 20%, the T_{T_2} values were higher than T_g. These observations suggest complex and concomitant phenomena influencing the T_2 values.

In order to better understand the mechanisms governing T_2, ratios of the mobile (B) and immobile (A) proton fractions (as determined using Eq. (1)) were plotted as a function of temperature for water contents between 15 and 35% (Fig. 6). The B/A ratio was nearly constant above 0 °C and up to 20 °C regardless of the water content. However, for higher water contents (RH = 91%), an increase in the B/A ratio was observed at 10 °C and 40 °C for the AX and BG films, respectively, which are very close to the T_g values observed for the two polymers (Table 2). This result shows that above T_g the motion of the polysaccharide chains in the rubbery state was so high that it influenced the mobile/immobile proton ratio and the measured T_2. This agrees with the decrease in the values of parameter a (calculated from Eq. (1)) measured for the films prepared at an RH of 91% (see M_2 determination). As a consequence, the apparent T_2 values should decrease significantly due to the combined contribution of motions from water and polysaccharide chains (Zimmerman & Brittin, 1957). This phenomenon has been proposed for models of relaxation under slow exchange between two sites with two different relaxation rates, $1/T_2$ (Zimmerman & Brittin, 1957).

However, for the samples at RH = 91%, the transition temperatures, T_{T_2}, estimated in Fig. 7 were 6–26 °C higher than the T_g, as was previously observed for T_{M_2} (see above). As already pointed out, a collapse phenomenon could induce a higher transition temperature as a consequence of intramolecular interactions that lower viscosity (Roos & Karel, 1990; Roos, 2002; Sato et al., 1983). Beyond this transition temperature, intra-molecular (or intra-chain) hydrogen bonds disrupt the induction of higher motions of the polysaccharide chains which then contribute to the mobile fraction causing B/A to increase. For samples with lower water content, the B/A increase should have occurred at temperatures exceeding 55 °C which was difficult to observe since the experiments were carried out only up to 80 °C (Figs. 6 and 7).

For samples with water contents below 20%, a transition temperature, T_{T_2}, lower than the T_g was observed (Table 2). In this case, the T_2 transition cannot be explained only by the additional contribution of motion from the polysaccharide protons. Below the T_g of the films, the mobile fraction that contributes to T_2 is thought to consist only of water protons with each of them being either bound to the polysaccharides through hydrogen bonds or free at high water content (Van den Dries et al., 1998). By increasing the water content within the films, the hydrogen bond stretches and the assembly properties of the polysaccharides weaken while the exchange of water molecules is favoured (Aeberhardt et al., 2007). Therefore, dipolar interactions between water and the hydroxyl groups of the polysaccharides are reduced and the rotational mobility of water is increased. As mentioned by Aeberhardt et al. (2007), the lifetime of a hydrogen bond is approximately as long as the transportation time of the water molecule from one hydrogen-bond acceptor site to another due to the proximity of other free acceptor sites in the glass state (below T_g). The probability that water is in a free state is therefore reduced in samples with low water content in a glassy state and diffusion should have no impact on the T_2 evolution.

Variation of the echo time in the CPMG experiment revealed no sigmoidal dispersion of $1/T_2$ relative to echo time (results not

shown) indicating in a first approximation that diffusion or chemical exchange had no influence on the T_2 measurements at 20 MHz. However, Hills, Wright, and Belton (1989) have used model systems (Sephadex beads) to show that combined diffusive and chemical exchanges can occur simultaneously. For some exchange rate, there is a timescale separation between the slow diffusive and fast chemical exchange processes (or the contrary) and therefore $1/T_2$ becomes constant against the echo time of CPMG (see Fig. 6 in Hills et al. (1989)). Further works involving measurements at a higher field could help to discriminate these processes by highlighting an eventual Larmor frequency dispersion.

Nevertheless, as the frequency of exchange rises with temperature, the probability that more than one water molecule is bound to one hydroxyl group at a given time increases. The maximum number of water molecules per hydroxyl group is close to 2 since the oxygen and hydrogen atoms of the hydroxyl groups can generate hydrogen bonds (Aeberhardt, de Saint Laumer, Bouquerand, & Normand, 2005). This probability is independent of the molecular weight of the oligosaccharide. An estimation of the number of water molecules per hydroxyl group can be done by calculating the number of exchangeable protons in the polysaccharides (n_{OH}) and water (n_H) in each of the samples using the following equations (Aeberhardt et al., 2007):

$$n_H = \frac{2}{18}\omega_w \tag{4}$$

$$n_{OH} = \frac{P_1}{P_2}(1 - \omega_w) \tag{5}$$

where P_1/P_2 corresponds to the proton density of the polysaccharides (8/132 for AX and 10/162 for BG) and ω_w is the weight fraction of water.

The amplitude of the FID signals is proportional to the proton density according to the following equations:

$$A = k_A \cdot n_{OH} \tag{6}$$

$$B = k_B \cdot n_H \tag{7}$$

where A and B correspond to the amplitude of the signal from the solid and liquid protons, respectively (previously determined fitting equation 1), k_A and k_B are proportionality constants and n_{OH} and n_H are the number of protons in the oligosaccharides and water, respectively.

k_A and k_B can be calculated at 20 °C if the water content is known (determined by sorption). These constants are directly linked to the energy absorbed by protons during the excitation of the solid and liquid protons and represent the average excitation state of the solid and liquid protons. If more than one water molecule binds to one hydroxyl group, there is equivalence in the bond energy and the water molecules are indistinguishable (Aeberhardt et al., 2007).

The k_B values calculated at 20 °C were 92 and 85 mA g mol^{-1} for AX and BG, respectively. These results are in agreement with the values determined for different oligosaccharides of $\overline{DP}_n$ between 7 and 46 (Aeberhardt et al., 2007). The k_A values were twice the values of k_B at 197 and 175 mA g mol^{-1} for AX and BG, respectively. The high value of k_A compared to k_B probably reflects the very high proton exchangeability of the hydroxyl group of polysaccharides, which can bind two water molecules, as indicated by the k_A/k_B ratio of 2. Therefore, at room temperature the apparent T_2 decrease is due to the reduced mobility of the water molecules that exhibit a higher probability to bind to the hydroxyl groups of the polysaccharide. At 80 °C, the k_A and k_B values were similar at around 82 mA g mol^{-1}, which suggests that only one water molecule binds to a hydroxyl group at high temperatures.

4. Conclusions

Our results point out the contribution of low-field NMR spectroscopy to the study of the mobility of polymer chains and their interactions with water in polysaccharide films. The transition temperatures measured by NMR, which is sensitive to high frequency motions, correlated well with the T_g values measured by DSC. Complementary mechanisms were emphasized, involving both the mobility of the polysaccharide chains below and above the glass transition temperature and the mobility of water molecules under the control of the frequency of exchange with hydroxyl groups of the polysaccharides. The results are consistent with stronger dipolar interactions between the protons in the BG films due to the shorter average distances between the linear chains of BG compared to the highly substituted chains of AX. BG chains are supposed to form a more compact structure with smaller nanopores than AX, which induces slower water mobility and kinetics of exchange. The different hydration properties observed for AX and BG films are of major importance in the context of the desiccation process for cereal grains. In addition to the heterogeneity of composition (AX/BG ratio), various structures of AX (A/X ratio) were also observed in endosperm tissues, but the impact of this compositional and structural heterogeneity on interactions with water or BG is unknown. NMR investigations as well as mechanical studies of films formulated with various amounts of BG and AX exhibiting different structural features are in progress in order to better understand their respective role in water transport in cereal grain.

Acknowledgments

The authors are indebted to the Regional Council of Pays de la Loire for financial support. They also thank Marion De Carvalho for the DSC analyses at INRA of Nantes. Access to the NMR facilities of the BIBS platform of INRA Angers-Nantes is acknowledged.

References

Abragam, A. (1961). *The principle of nuclear magnetism*. Oxford: Clarendon Press.
Aeberhardt, K., Bui, Q. D., & Normand, V. R. (2007). Using low-field NMR to infer the physical properties of glassy oligosaccharide/water mixtures. *Biomacromolecules*, *8*, 1038–1046.
Aeberhardt, K., de Saint Laumer, J.-Y., Bouquerand, P.-E., & Normand, V. (2005). Ultrasonic wave spectroscopy study of sugar oligomers and polysaccharides in aqueous solutions: The hydration length concept. *International Journal of Biological Macromolecules*, *36*(*5*), 275–282.
Bacic, A., & Stone, B. A. (1981). Chemistry and oraganization of aleurone cell wall components from wheat and barley. *Australian Journal of Plant Physiology*, *8*, 475–495.
Barron, C., Parker, M. L., Mills, E. N. C., Rouau, X., & Wilson, R. H. (2005). FT-IR imaging of wheat endosperm cell walls in situ reveals compositional and architectural heterogeneity related to grain hardness. *Planta*, *220*, 667–677.
Bloembergen, N., Purcell, E. M., & Pound, R. V. (1948). Relaxation effects in nuclear magnetic resonance absorption. *Physical Review*, *73*, 679–712.
Bradford, M. M. (1976). A rapid and sensitive method for the quantization of microgram quantities of protein utilizing the principle of protein–dye binding. *Analytical Biochemistry*, *72*, 248–255.
Buliga, G. S., Brant, D. A., & Fincher, G. B. (1986). The sequence statistics and solution conformation of a barley (1-3, 1-4)-beta-D-glucan. *Carbohydrate Research*, *157*, 139–156.
Ciacco, C. F., & d'Appolonia, B. L. (1982). Characterization and gelling capacity of water-soluble pentosans isolated from different mill streams. *Cereal Chemistry*, *59*, 163–166.
Cornillon, P., & Salim, L. C. (2000). Characterization of water mobility and distribution in low and intermediate-moisture food systems. *Magnetic Resonance Imaging*, *18*, 335–341.
Cui, W., Wood, P. J., Blackwell, B., & Nikiforuk, J. (2000). Physicochemical properties and structural characterization by two-dimensional NMR spectroscopy of wheat beta-D-glucan comparison with other cereal beta-D-glucans. *Carbohydrate Polymers*, *41*, 249–258.
Dais, P., & Perlin, A. S. (1982). High-field, C-13-Nmr spectroscopy of β-D-glucans, amylopectin, and glycogen. *Carbohydrate Research*, *100*, 103–116.
Derbyshire, W., van den Bosch, M., van Dusschoten, D., MacNaughtan, W., Farhat, I. A., Hemminga, M. A., et al. (2004). Fitting of the beat pattern observed in NMR free-

induction decay signals of concentrated carbohydrate–water solutions. *Journal of Magnetic Resonance*, *168*, 278–283.
Dervilly, G., Saulnier, L., Roger, P., & Thibault, J. F. (2000). Isolation of homogeneous fractions from wheat water-soluble arabinoxylans. Influence of the structure on their macromolecular characteristics. *Journal of Agricultural and Food Chemistry*, *48*, 270–278.
Dervilly-Pinel, G., Rimsten, L., Saulnier, L., Andersson, R., & Aman, P. (2001). Water-extractable arabinoxylan from pearled flours of wheat, barley, rye and triticale. Evidence for the presence of ferulic acid dimers and their involvement in gel formation. *Journal of Cereal Science*, *34*, 207–214.
Dervilly-Pinel, G., Tran, V., & Saulnier, L. (2004). Investigation of the distribution of arabinose residues on the xylan backbone of water-soluble arabinoxylans wheat flour. *Carbohydrate Polymers*, *55*, 171–177.
Ediger, M. D., Angell, C. A., & Nagel, S. R. (1996). Supercooled liquids and glasses. *Journal of Physical Chemistry*, *100*, 13200–13212.
Englyst, H. N., & Cummings, J. H. (1988). Improved method for measurement of dietary fibre as non-starch polysaccharides in plant foods. *Journal of the Association of Official Analytical Chemists*, *71*, 808–814.
Fincher, G. B., & Stone, B. A. (1986). Cell walls and their components in cereal grain technology. *Advances in Cereal Science and Technology*, *8*, 207–295.
Fulcher, R. G., Miller, S. S., & Ruan, R. (1997). Quantitative microscopic approaches to carbohydrate characterization and distribution in cereal grains. In T. Johns, & J. T. Romeo (Eds.), *Functionality of food phytochemicals* (pp. 237–261). New York: Plenum.
Goodman, A. M. (1978). Optical interference method for the approximate determination of refractive index and thickness of a transparent layer. *Applied Optics*, *17*, 2779–2787.
Gottwald, A., Creamer, L. K., Hubbard, P. L., & Callaghan, P. T. (2005). Diffusion, relaxation, and chemical exchange in casein gels: A nuclear magnetic resonance study. *Journal of Chemical Physics*, *122*, 034506–34511.
Greenspan, L. (1977). Humidity fixed points of binary saturated aqueous solutions. *Journal of Research of the National Bureau of Standards Section A – Physics and Chemistry*, *81*, 89–96.
Guillon, F., Tranquet, O., Quillien, L., Utille, J. P., Ordaz Ortiz, J. J., & Saulnier, L. (2004). Generation of polyclonal and monoclonal antibodies against arabinoxylans and their use for immunocytochemical location of arabinoxylans in cell walls of endosperm of wheat. *Journal of Cereal Science*, *40*, 167–182.
Hills, B. P., Wright, K. M., & Belton, P. S. (1989). Proton NMR-studies of chemical and diffusive exchange in carbohydrates systems. *Molecular Physics*, *67*, 1309–1326.
Hoffmann, R. A., Roza, M., Maat, J., Kamerling, J. P., & Vliegenthart, J. F. G. (1991). Structural characterisation of the cold water-soluble arabinoxylans from the white flour of the soft wheat variety kadet. *Carbohydrate Polymers*, *15*, 415–430.
Hoije, A., Sternemalm, E., Heikkinen, S., Tenkanen, M., & Gatenholm, P. (2008). Material properties of films from enzymatically tailored arabinoxylans. *Biomacromolecules*, *9*, 2042–2047.
Izawa, M., Kano, Y., & Koshino, S. (1993). Relationship between structure and solubility of (1-3, 1-4)-beta-D-glucan from barley. *Journal of the American Society of Brewing Chemists*, *51*, 123–127.
Izydorczyk, M. S., & Biliaderis, C. G. (1994). Studies on the structure of wheat endosperm arabinoxylans. *Carbohydrate Polymers*, *24*, 61–71.
Izydorczyk, M. S., & Biliaderis, C. G. (1995). Cereal arabinoxylans: Advances in structure and physicochemical properties. *Carbohydrate Polymers*, *28*, 33–48.
Izydorczyk, M. S., Macri, L. J., & MacGregor, A. W. (1998a). Structure and physicochemical properties of barley non-starch polysaccharides – I. Water-extractable beta-glucans and arabinoxylans. *Carbohydrate Polymers*, *35*, 249–258.
Izydorczyk, M. S., Macri, L. J., & MacGregor, A. W. (1998b). Structure and physicochemical properties of barley non-starch polysaccharides – II. Alkali-extractable beta-glucans and arabinoxylans. *Carbohydrate Polymers*, *35*, 259–269.
Izydorczyk, M. S., & McGregor, A. W. (2000). Evidence of intermolecular interactions of β-glucans and arabinoxylans. *Carbohydrate Polymers*, *41*, 417–420.
Kilburn, D., Claude, J., Schweizer, T., Alam, A., & Ubbink, J. (2005). Carbohydrate polymers in amorphous states: An integrated thermodynamic and nanostructural investigation. *Biomacromolecules*, *6*, 864–879.
Kumagai, H., MacNaughtan, W., Farhat, I. A., & Mitchell, J. R. (2002). The influence of carrageenan on molecular mobility in low moisture amorphous sugars. *Carbohydrate Polymers*, *48*, 341–349.
MacGregor, A. W., & Fincher, G. B. (1993). Carbohydrates of the barley grain. In A. W. MacGregor, & R. S. Bhatty (Eds.), *Barley: Chemistry and technology* (pp. 73–130). St. Paul, MN: AACC.
Mansfield, M. L. (1993). In J. M. V. Blanshard, & P. J. Lillford (Eds.), *The glassy state in foods* (pp. 103–122). Loughborough: Nottingham University Press.
Marquardt, D. W. (1963). An algorithm for least-squares estimation of nonlinear parameters. *SIAM Journal on Applied Mathematics*, *11*, 431–441.
Meiboom, S., & Gill, D. (1958). Modified spin-echo method for measuring nuclear relaxation times. *Review of Scientific Instruments*, *29*, 688–691.
Partanen, R., Marie, V., MacNaughtan, W., Forssell, P., & Farhat, I. (2004). H-1 NMR study of amylose films plasticised by glycerol and water. *Carbohydrate Polymers*, *56*, 147–155.
Philippe, S., Barron, C., Robert, P., Devaux, M. F., Saulnier, L., & Guillon, F. (2006). Characterization using Raman microspectroscopy of arabinoxylans in the walls of different cell types during the development of wheat endosperm. *Journal of Agricultural and Food Chemistry*, *54*, 5113–5119.
Philippe, S., Robert, P., Barron, C., Saulnier, L., & Guillon, F. (2006). Deposition of cell wall polysaccharides in wheat endosperm during grain development: Fourier transform-infrared microspectroscopy study. *Journal of Agricultural and Food Chemistry*, *54*, 2303–2308.
Philippe, S., Saulnier, L., & Guillon, F. (2006). Arabinoxylan and (1 → 3), (1 → 4)-β-glucans deposition in cell walls during wheat endosperm development. *Planta*, *224*, 449–461.
Philippe, S., Tranquet, O., Utille, J. P., Saulnier, L., & Guillon, F. (2007). Investigation of ferulate deposition in endosperm cell walls of mature and developing wheat grains by using a polyclonal antibody. *Planta*, *225*, 1287–1299.
Provencher, S. W. (1982). CONTIN: A general purpose constrained regularization program for inverting noisy linear algebraic and integral equations. *Computer Physics Communications*, *27*, 229–242.
Rattan, O., Izydorczyk, M. S., & Biliaderis, C. G. (1994). Structure and rheological behaviour of arabinoxylans from Canadian bread wheat flours. *Lebensmittel-Wissenschaft and Technologie*, *27*, 550–555.
Rondeau-Mouro, C., Defer, D., Leboeuf, E., & Lahaye, M. (2008). Assessment of cell wall porosity in Arabidopsis thaliana by NMR spectroscopy. *International Journal of Biological Macromolecules*, *42*, 83–92.
Roos, Y., & Karel, M. (1990). Differential scanning calorimetry atudy of phase-transitions affecting the quality of dehydrated materials. *Biotechnology Progress*, *6*, 159–163.
Roos, Y. H. (2002). Importance of glass transition and water activity to spray drying and stability of dairy powders. *Lait*, *82*, 475–484.
Roudaut, G., Farhat, I., Poirier-Brulez, F., & Champion, D. (2009). Influence of water, temperature and sucrose on dynamics in glassy starch-based products studied by low field H-1 NMR. *Carbohydrate Polymers*, *77*, 489–495.
Ruan, R. R., & Chen, P. L. (1998). *Water in foods and biological materials. A nuclear magnetic resonance approach*. Lancaster, PA: Technomic Publishing. , p. 298.
Sato, T., Sakurai, K., Norisuye, T., & Fujita, H. (1983). Triple helix of schizophyllum-commune polysaccharide in dilute-solution.6. Collapse of randomly coiled schizophyllan in mixtures of water and dimethylsulfoxide. *Polymer Journal*, *15*, 87–96.
Saulnier, L., Vigouroux, J., & Thibault, J.-F. (1995). Isolation and characterization of feruloylated oligosaccharides from maize bran. *Carbohydrate Research*, *272*, 241–253.
Saulnier, L., Sado, P.-E., Branlard, G., Charmet, G., & Guillon, F. (2007). Wheat arabinoxylans: Exploiting variation in amount and composition to develop enhanced varieties. *Journal of Cereal Science*, *46*, 261–281.
Staudte, R. G., Woodward, J. R., Fincher, G. B., & Stone, B. A. (1983). Water-soluble (1–3), (1–4)-β-D-glucans from barley (Hordeum vulgare) endosperm. III: Distribution of cellotriosyl and cellotetraosyl residues. *Carbohydrate Polymers*, *3*, 299–312.
Tvaroska, I., Ogawa, K., Deslandes, Y., & Marchessault, R. H. (1983). Crystalline conformation and structure of lichenan and barley beta-glucan. *Canadian Journal of Chemistry*, *61*, 1608–1616.
Van den Dries, I. J., Besseling, N. A. M., Van Dusschoten, D., Hemminga, M. A., & Van der Linden, E. (2000). Relation between a transition in molecular mobility and collapse phenomena in glucose-water systems. *The Journal of Physical Chemistry B*, *104*, 9260–9266.
Van den Dries, I. J., Van Dusschoten, D., Hemminga, M. A., & Van der Linden, E. (2000). Effects of water content and molecular weight on spin probe and water mobility in malto-oligomer glasses. *Journal of Physical Chemistry B*, *104*, 10126–10132.
Van den Dries, I. J., Van Dusschoten, D., & Hemminga, M. A. (1998). Mobility in maltose-water glasses studied with H-1 NMR. *The Journal of Physical Chemistry B*, *102*, 10483–10489.
Wood, P. J., Weisz, J., & Blackwell, B. A. (1991). Molecular characterization of cereal beta-D-glucans – structural-analysis of oat beta-D-glucan and rapid structural evaluation of beta-D-glucans from different sources by high-performance liquid-chromatography of oligosaccharides released by lichenase. *Cereal Chemistry*, *68*, 31–39.
Wood, P. J., Weisz, J., & Blackwell, B. A. (1994). Structural studies of (1-3), (1-4)-beta-D-glucans by C(13)-nuclear magnetic-resonance spectroscopy and by rapid analysis of cellulose-like regions using high-performance anion-exchange chromatography of oligosaccharides released by lichenase. *Cereal Chemistry*, *71*, 301–307.
Zimmerman, J. R., & Brittin, W. E. (1957). Nuclear magnetic resonance studies in multiple phase systems: Lifetime of a water molecule in an adsorbing phase on silica gel. *Journal of Physical Chemistry*, *61*, 1328–1333.